

RSC Advances



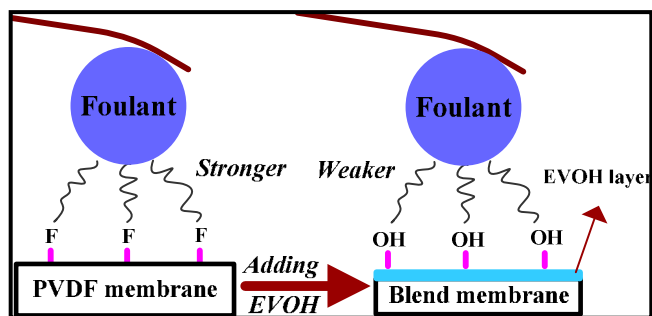
This is an *Accepted Manuscript*, which has been through the Royal Society of Chemistry peer review process and has been accepted for publication.

Accepted Manuscripts are published online shortly after acceptance, before technical editing, formatting and proof reading. Using this free service, authors can make their results available to the community, in citable form, before we publish the edited article. This *Accepted Manuscript* will be replaced by the edited, formatted and paginated article as soon as this is available.

You can find more information about *Accepted Manuscripts* in the [Information for Authors](#).

Please note that technical editing may introduce minor changes to the text and/or graphics, which may alter content. The journal's standard [Terms & Conditions](#) and the [Ethical guidelines](#) still apply. In no event shall the Royal Society of Chemistry be held responsible for any errors or omissions in this *Accepted Manuscript* or any consequences arising from the use of any information it contains.

Graphical Abstract



The antifouling ability of the PVDF/EVOH blended membrane is superior to that of the PVDF membrane

ARTICLE

Polyvinylidene fluoride/poly(ethylene-co-vinyl alcohol) blended membranes and a systematic insight into their antifouling property

Rui Miao, Lei Wang*, Zhe Gao, Na Mi, Tingting Liu, Yongtao Lv, Xudong Wang

ABSTRACT: PVDF/EVOH (P/E) membranes were prepared via immersion precipitation to realize an antifouling property better than that of PVDF membranes. To determine the optimum conditions for preparing a P/E blended membrane, the effects of the P/E weight ratio and temperature of the coagulation bath on the properties of the blended membrane were investigated. The fouling behaviors and membrane–foulant interaction force of the P/E blended membrane were compared with those of a PVDF membrane for unraveling its antifouling ability. Results show that the P/E membrane appeared to be more hydrophilic, having a higher pure-water flux and bovine serum albumin rejection rate than the PVDF membrane. The integrated performance of the P/E membrane was best when the P/E weight ratio and temperature of the coagulation bath were fixed at 9/1 and 20 °C, respectively. Analysis of the antifouling ability revealed that the flux decline rate of the P/E membrane were much less than those of the PVDF membrane. This phenomenon, combined with the measurements of the membrane–foulant interaction force, demonstrate that the membrane–fouling interaction force was reduced by the addition of EVOH, which could weaken the adsorption and accumulation of foulants on the membrane surface or pores and reduce the rate of membrane flux decline.

1. Introduction

Wastewater reuse and reclamation are increasingly being emphasized as a strategy for resolving water shortages and preventing deterioration of the aquatic environment through wastewater disposal.^{1,2} Ultrafiltration (UF) membrane technology has attracted increasing attention in the field of wastewater reuse and reclamation because it offers remarkable advantages relating to effluent quality and a reduced footprint compared with conventional processes.^{3,4}

UF membranes are generally synthesized with such polymers as polysulfone, polyethersulfone, polypropylene and polyvinylidene fluoride (PVDF).⁵ Among these polymers, PVDF is one of the most extensively applied membrane materials in UF systems owing to its excellent antioxidation properties, thermal stability, chemical resistance and high mechanical strength.⁶ However, the highly hydrophobic nature of PVDF often leads to low water flux and the adsorption of organic matter (such as sodium alginate and humic acid) on the

surface or pores of PVDF membranes, which results in severe membrane fouling and has become a conspicuous drawback for the further application of PVDF membranes in water treatment.^{7–9} Therefore, hydrophilic modification is an effective strategy for improving the antifouling ability of PVDF membranes.¹⁰

As a major modification strategy, the blending of hydrophilic polymers is a simple and efficient way of enhancing the hydrophilicity of PVDF membranes.¹¹ Employing this method, hydrophilic polymers are usually introduced into PVDF membranes during phase separation without any pretreatment or posttreatment procedures. The main hydrophilic blending materials used include polyvinyl alcohol, polyvinyl pyrrolidone, and polyethylene glycol. However, it should be noted that the above polymers are water soluble, and can be washed out of the matrix during membrane preparation and operation.¹² Researchers have reported that water-insoluble hydrophilic polymers (e.g., polymethyl methacrylate, sulfonated polycarbonate, and perfluorosulfonic acid) can be blended into a PVDF matrix to effectively improve its hydrophilicity.^{13–15} Therefore, choosing an appropriate blend of water-insoluble hydrophilic polymers and PVDF is an effective strategy for improving the permanent hydrophilicity of the PVDF membrane.

School of Environmental & Municipal Engineering, Xi'an University of Architecture and Technology, Yan Ta Road, No.13, Xi'an 710055, China.

A poly(ethylene-co-vinyl alcohol) (EVOH) chemical chain has a large number of hydrophilic hydroxyl groups and good wet strength and hydrophilicity. Furthermore, EVOH is a water-insoluble polymer. Recently, the EVOH membrane has attracted attention from membrane research groups around the world in the field of wastewater treatment.^{16,17} EVOH/polyvinyl pyrrolidone blended membranes were successfully prepared employing nonsolvent-induced phase inversion and their formation mechanism was investigated.¹⁶ Lima et al. prepared microporous EVOH/poly(methyl methacrylate) blended membranes by thermally induced phase separation.¹⁸ However, little of the literature has focused on the preparation, performance or application of EVOH membranes. This is because there is a high density of hydroxyls in EVOH chains, allowing both inter- and intramolecular hydrogen interactions between these hydroxyls and resulting in EVOH having limited miscibility with other polymers.^{17,18} In addition, EVOH membranes possess poor mechanical strength. These disadvantages of EVOH are mainly responsible for the limited use of EVOH as a membrane material. It is worth noting that the hydrophilicity, poor mechanical strength and weak compatibility of EVOH contrast with the PVDF properties of hydrophobicity, good mechanical strength and strong compatibility with other polymers.¹⁹

Moreover, PVDF possesses the most electronegative element, namely fluoride. A hydrogen bond forms by electron transfer between electronegative fluorine atoms (from the PVDF membrane) and hydrogen atoms (from the hydroxyl group of EVOH),²⁰ which could enhance the compatibility of PVDF with EVOH. We thus propose to blend PVDF and EVOH, which have complementary properties, to mitigate the hydrophobic and antifouling properties of PVDF membranes.

The purpose of this study was to synthesize PVDF/EVOH (P/E) blended membranes by immersion precipitation. Effects of the P/E weight ratio and the temperature of the coagulation bath on the properties of the blended membrane were systematically investigated by examining the performances of blended membranes in terms of pure-water flux, morphological structure, mechanical properties and hydrophilicity. In addition, fouling experiments with sodium alginate (SA) and humic acid (HA) wastewater were carried out using PVDF and selected P/E blended UF membranes. Hydroxyl and carboxyl colloidal probes were used as surrogates of SA-like substances and HA-like substances, respectively, in conjunction with atomic force microscopy (AFM) to measure the adhesion forces between PVDF and SA/HA and between P/E blended membranes and SA/HA. We combined this analysis with corresponding fouling experiments to assess the antifouling ability of the PVDF membrane and the P/E blended membrane. The ultimate goal is to provide a theoretical basis for the preparation and application of P/E blended membranes in the reuse of wastewater.

2. Experimental

2.1. Materials

2.1.1. Membrane materials

Polyvinylidene fluoride (PVDF; Solef 1015, Solvay Advanced Polymers Co., America), polyethyleneco-vinyl alcohol (EVOH; ethylene content of 32%, Kuraray Japan), N,N-

dimethylecetamide (DMAc; Tianjin Fuchen Chemical Reagent Co., China), lithium chloride (LiCl, Tianjin Chemical Reagent Co., China) and bovine serum albumin (BSA, Sigma-Aldrich, St. Louis, MO, $M_w = 6.7$ kDa) were used as membrane materials.

2.1.2. Organic foulants

Commercial sodium alginate (SA, Sigma-Aldrich, St. Louis, Mo) and humic acid (HA, Sigma-Aldrich, St. Louis, Mo) were used as model organic foulants to represent the polysaccharide-like and humus-like substances in wastewater, respectively. HA and SA (1g/L) stock solutions were prepared and filtered with 0.45 μ m microfiltration membranes to remove particulate and insoluble matter and then stored in sterilized glass bottles at 4 °C prior to use.

2.2. P/E membrane fabrication

PVDF and P/E blended membranes were synthesized via immersion precipitation. In brief, certain amounts of PVDF, EVOH and LiCl were dissolved in DMAc at room temperature, heated to 60 °C while being vigorously stirred and left for 16 h to obtain a homogeneous solution. The homogeneous solution was then allowed to stand for 6–8 h to allow air bubbles to escape. The resulting homogeneous polymer solution was uniformly spread onto a glass plate using a casting knife; the glass plate with the cast solution was then immediately immersed into a coagulation bath (deionized water) having constant temperature. The membrane precipitated on the glass plate. The membrane was thoroughly rinsed and then immersed in deionized water for 4–5 days to remove residual solvent.

2.3. Permeation measurements

A dead-end filtration setup as previously described in the literature was used for the permeation tests.²¹ The test unit mainly comprised a N₂ cylinder, a stirred cell (used to hold the feed solution and the test membrane), a magnetic stirring apparatus and an electronic balance. The membrane sample was placed in the bottom of the stirred cell. Constant pressure was applied throughout the filtration period using a compressed N₂ cylinder with a pressure gauge. The permeate flux data were continuously recorded using an electronic balance connected to a computer.

2.3.1. Pure-water flux

The membranes prepared by immersion precipitation were cut into discs with an effective filtration area of 28 cm² for the filtration setup. A new membrane sample was firmly fixed to the bottom of the stirred cell. Firstly, the membrane was precompacted with deionized water under 0.15 MPa until the permeate flux became stable. The transmembrane pressure was then lowered to 0.10 MPa and the membrane was stabilized with deionized water for 30 min to establish a stable permeate flux that is referred to as the pure-water flux (J_0). The pure-water flux was calculated from the volume of the water permeate per unit time and unit area of the membrane surface as follows:

$$J_0 = \frac{V}{S \cdot t}, \quad (1)$$

where J_0 (L·m⁻²·h⁻¹) is the pure-water flux of the membrane, V (L) is the volume of permeated water, S (m²) is the effective membrane area and t (h) is the permeation time.

2.3.2. BSA rejection studies

BSA was used as a standard material to test the rejection of the membranes under filtration conditions. The feed concentration of the BSA solution was 0.1 g/L (pH = 7.0±0.2) and the permeated solution was gathered. The concentration of the BSA solution was determined from the absorbance recorded by an ultraviolet spectrophotometer at a wavelength of 280 nm. Rejection of BSA was calculated as:

$$\text{Rejection} = \left(1 - \frac{C_p}{C_0}\right) \times 100\%, \quad (2)$$

where C_0 and C_p are the concentrations of BSA in the feed and permeate solutions, respectively.

2.4. Membrane filtration experiments

PVDF and P/E ultrafiltration membrane fouling experiments were performed with HA and SA solution using a dead-end cell membrane filtration setup as described in Section 2.3. To avoid a concentration effect, the concentrations of dissolved organic carbon of all foulant solutions (pH = 7.0) were reduced to the same value of 10 mg/L. A new membrane was used in each experiment. First, the pure-water flux (J_0) of the new membrane was measured. The SA or HA solution was then filtered through the membrane under a pressure of 0.10 MPa for 30 min, and at this stage changes in the membrane flux (J) were monitored online.

2.5. AFM adhesion force measurements

Humic-like and polysaccharide-like substances are the organic matter most commonly found in wastewater, and are the two major types of membrane foulants.²² Therefore, unraveling the fouling behavior of humic-like and polysaccharide-like substances is crucial to applying membranes in wastewater treatment. In addition, HA and SA are typical humic-like and polysaccharide-like substances, and are thus rich in carboxyl and hydroxyl groups, respectively. Therefore, in this study, carboxyl-group and hydroxyl-group colloidal probes were prepared and used as surrogates of HA and SA, respectively. The interaction forces between PVDF or the P/E membrane and the colloidal probe were determined by AFM in conjunction with the corresponding colloidal probe.

A microscope (TH4-200; Olympus, Japan) was used to magnify the operational space and to continuously monitor the preparation of the probe. First, a small drop of Epikote was adsorbed onto the surface of the cantilever free end of a tipless AFM probe (NP-10; Bruker, Germany) with the aid of a manipulator (World Precision Instruments Co., KITE-L, USA). A carboxyl or hydroxyl microsphere with a diameter of 5 μm was then attached to the end of the cantilever via the Epikote. Finally, colloidal probes were stored at 4 °C for at least 48 h prior to use.

A MultiMode 8.0 atomic force microscope (Bruker, Germany) in conjunction with carboxyl or hydroxyl colloidal probes was used to quantify the interaction forces between the corresponding colloidal probe and PVDF or P/E blended membrane. The AFM measurements of the interaction force were made in a fluid cell using a closed inlet/outlet loop as follows. Unless otherwise specified, all AFM measurements were carried out in buffer solution (1 mM NaHCO_3 , pH 7.8) in contact mode. First, a membrane sample (PVDF or P/E

membrane) was mounted in the bottom of the fluid cell and then rinsed with the buffer solution at least three times. The force between the membrane and foulant (carboxyl or hydroxyl) was measured with a carboxyl or hydroxyl colloidal probe after the fluid cell was fully filled with the buffer solution. For each type of membrane sample, force measurements were made at six locations, and more than 10 force curves were obtained at each location. To ensure accuracy of the force measurements, the integrity of the colloidal probe was carefully examined by scanning electron microscopy (SEM) before and after each use. For each type of interaction force, nearly 100 force curves were obtained, and it was found that the force values were not exactly equal to each other. Therefore, the frequency distributions of the corresponding forces were calculated to provide a clear distribution of maximum adhesion forces at a glance.

2.6. Analytical technology

A MultiMode 8.0 AFM instrument equipped with a NanoScope V controller (Bruker) was used to measure the surface morphology of ultrafiltration membranes. SEM (JSM5800, Japan) was employed to characterize the cross-section morphology of the membranes. The contact angle of the membrane surface was determined using a contact angle analyzer (SL200B, USA Kino Industry Ltd.). An electronic yarn strength apparatus (HD021NS, Nantong Honda Experiment Instruments Co., Ltd., China) was used to determine the mechanical strength of the UF membrane. The concentration of dissolved organic carbon in each foulant solution sample was measured by a TOC analyzer (TOC-L, CPNk Shimadzu, Japan). All measurement experiments were performed at least five times to minimize test error, reproducibility is satisfactory.

3. Results and discussion

3.1. Effect of the P/E mass ratio on the properties of the blended membrane

To better understand the effect of the P/E mass ratio on the properties of the blended membrane, P/E blended membranes with a mass ratio of PVDF to EVOH of 20/0, 19/1, 9/1 and 17/3 (the total polymer content of the casting solution was 20) were prepared and their properties analyzed. The temperature of the coagulation bath was fixed at 20 °C. The quantities of EVOH in the P/E mixture solution did not increase further, mainly because the homogeneity of the casting solution deteriorated as the P/E mass ratio reached 17/3.

3.1.1. Morphology of membranes with different EVOH content in the casting solution

To better understand the changes in the membrane pore size and pore density before and after blending EVOH, the cross-section morphology of PVDF and P/E blended membranes with different EVOH content in the casting solution were characterized by SEM; results are shown in Fig. 1. It is evident that the PVDF membrane and all P/E blended membranes have a typically asymmetric structure comprising a skin top layer and a porous sublayer. Nevertheless, there is

ARTICLE

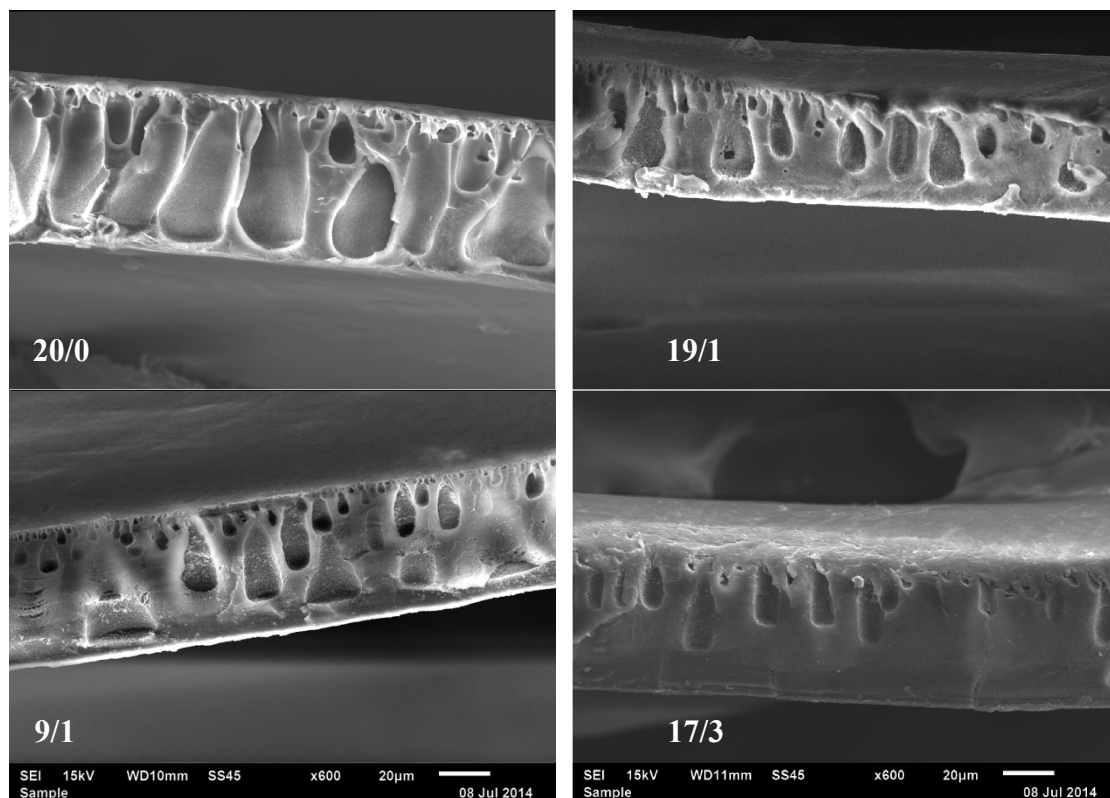


Figure 1. SEM images of a cross section prepared by immersion precipitation with different EVOH content in the casting solution.

an important difference between the morphology of the PVDF membrane and that of the P/E blended membrane. The PVDF membrane has finger-like cavities and all the pores in its sublayer are fully developed. However, the quantity and size of the finger-like cavities beneath the skin layer of the membrane reduced sharply once EVOH was introduced. Moreover, with an increase in EVOH content in the casting solution, the pore size and pore density in the cross section of the membrane decreased continuously, while the thickness of the skin layer increased. This change in the membrane morphology with an increase in the EVOH content in the casting solution may result from hydrophilic EVOH migrating spontaneously to the membrane/water interface during the phase inversion and an EVOH skin layer developing as the separation of the membrane phase finishes.²³ This phenomenon continues to intensify with an increase in the EVOH content in the casting solution. However, with an increase in the EVOH content in the casting solution, the chances of a pore formation agent migrating to the coagulation phase reduces because of competing EVOH migration, and the pore size and pore density in the cross section of the membrane thus gradually reduce.

3.1.2. Effect of the P/E mass ratio on hydrophilicity and mechanical strength

Figure 2 shows the contact angles and mechanical strengths of blended membranes having different P/E mass ratios. It is

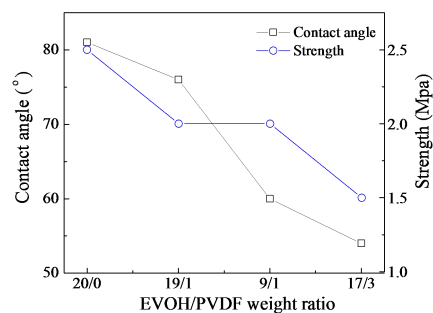


Figure 2. Contact angle and mechanical strength of blended membranes with different P/E mass ratios.

clearly demonstrated that the contact angles of the blended membranes gradually decreased as the amount of EVOH in the blended membranes increased; i.e., the hydrophilicity of the PVDF membrane was improved by adding EVOH. This phenomenon can be explained by the fact that during the phase inversion, the hydrophilic parts of EVOH migrated spontaneously to the membrane/water interface to reduce the

interface energy, and the accumulation of EVOH on the blended membrane surface reduced the contact angle.²³ Furthermore, with an increase in the EVOH content in the blended membranes, the accumulated dose of EVOH on the blended membrane surface increased, which reduced the contact angle of the corresponding blended membrane.

It is also seen that the mechanical strength tended to decrease as the amount of EVOH increased in the blended membranes. This was mainly due to the high density of hydroxyls in the EVOH chains allowing both inter- and intramolecular hydrogen interactions between these hydroxyls, which resulted in the EVOH having limited miscibility with other polymers.¹⁸ Therefore, the extent of self-aggregation of EVOH increased with an increase in the EVOH content in the blended membranes. This would cause a nonuniform distribution of EVOH in the P/E matrix, providing weak links between PVDF and EVOH and thereby reducing the mechanical strength of the P/E blended membrane.²⁴

3.1.3. Permeation performance of P/E blended membranes with different P/E mass ratios

The pure-water flux and BSA rejection of blended membranes as a function of the P/E mass ratio are illustrated in Figure 3. It is clearly demonstrated that the BSA rejection

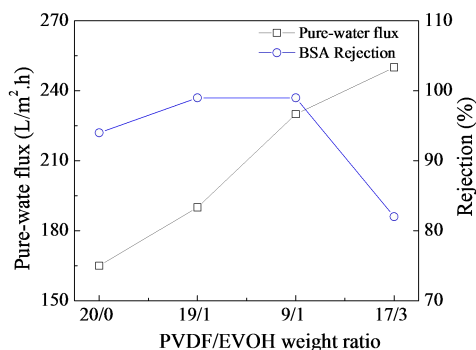


Figure 3. Effects of the P/E mass ratio on the pure-water flux and BSA rejection of P/E blended membranes.

reached 99% for blended membranes with P/E mass ratios of 19/1 and 9/1, while the membrane prepared without EVOH had a lower BSA rejection of 94%. This may be due to the hydrophilic EVOH migrating continuously and aggregating at the membrane/water interface during the phase inversion, thus reducing the rate of migration of the pore-forming agent into the water phase. This would reduce the pore size and pore density of the blended membranes and increase BSA rejection. However, the BSA rejection declined sharply to 80% for the blended membrane with a P/E mass ratio of 17/3. This may be because the compatibility between PVDF and EVOH worsens dramatically as the P/E mass ratio increases to 17/3, which could greatly increase the drawbacks of using P/E blended membranes and decrease the BSA rejection by the membranes.

The PVDF membrane had the lowest pure-water flux value of 160 L/m².h, while the pure-water flux values of P/E

blended membranes with mass ratios of 19/1, 9/1 and 17/3 P/E were 190, 230 and 250 L/m².h, respectively. Obviously, the pure-water flux of P/E blended membranes gradually increased with an increase in the EVOH content in blended membranes. It is generally accepted that the water permeation of a membrane is mainly controlled by the hydrophilicity and structure of the membrane.²⁵ The hydrophilic membrane surface is easily wetted by water, which promotes the passage of water molecules through the membrane. In addition, increases in pore size and pore density improve the water permeation but reduce BSA rejection through the membranes.²⁶ Analysis of the cross-section morphology of membranes reveals that the pore size and pore density of the membranes reduced with an increase in the EVOH content of the blended membranes. Additionally, the pure-water flux of blended membranes increased with an increase in the EVOH content. This suggests that the pure-water flux increase of P/E blended membranes is the result of improved membrane hydrophilicity.

On the basis of the above analysis, it is clear that the hydrophilicity and pure-water flux of membranes increase with an increase in EVOH content. However, the mechanical strength and BSA rejection declined sharply when the EVOH content reached a maximum (17/3). The optimum P/E mass ratio is 9/1 when the hydrophilicity, mechanical strength, pure-water flux and BSA rejection of P/E blended membranes with different EVOH content in the casting solution are taken into account.

3.2. Effect of the temperature of the coagulation bath on membrane properties

3.2.1. Surface morphology of the P/E blended membrane at different temperatures of the coagulation bath

The surface morphology of the P/E blended membrane at different temperatures of the coagulation bath was characterized by AFM. Figure 4 shows two-dimensional and three-dimensional AFM images of the P/E blended membrane with a PVDF/EVOH mass ratio of 9/1 prepared at different temperatures of the coagulation bath. It is observed that the surface homogeneity of the P/E blended membrane increase with an increase in the temperature of the coagulation bath, while the pore density is noticeably reduced. In particular, as the temperature of the coagulation bath increases from 20 to 40 °C, the surface morphology of the P/E blended membrane changes remarkably; the membrane surface becomes smoother and a uniform distribution of pores forms on the membrane surface. The pore size and pore density of the blended membrane decrease further as the temperature of the coagulation bath increases to 60 °C. These observations are consistent with the findings of Conesa et al., who reported that the membrane pore size and pore density decrease with increasing temperature of the coagulation bath.^{27,28} This phenomenon may be explained by the difference in demixing mechanisms between lower and higher temperatures of the coagulation bath. At a higher temperature, the exchange of the solvent and nonsolvent is expedited, and a dense top skin then forms and instantaneously hinders the exchange, thus reducing the pore size and pore density.²⁹

ARTICLE

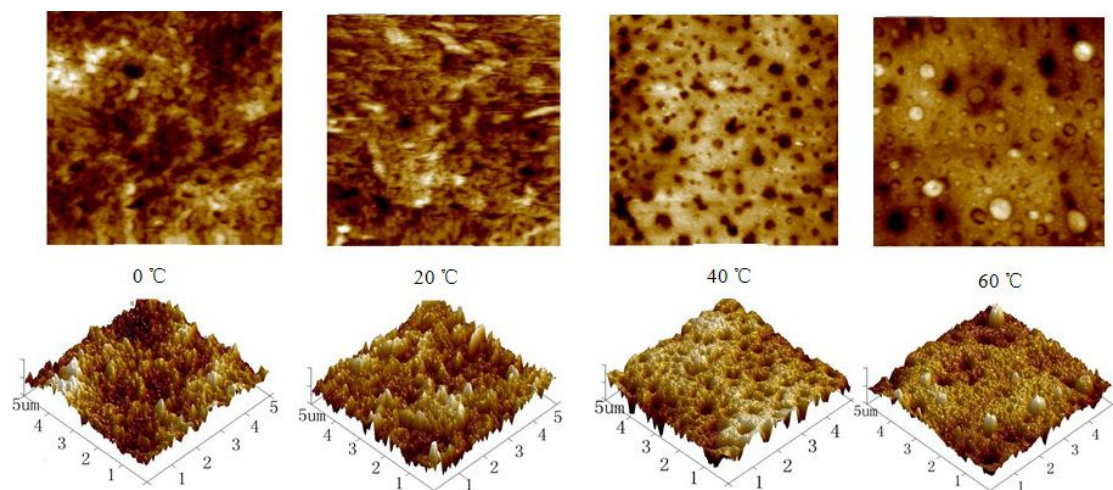


Figure 4. Surface morphology of the P/E blended membrane at different temperatures of the coagulation bath.

3.2.2. Hydrophilicity of membranes prepared at different temperatures of the coagulation bath

Table 1 presents the water contact angles of the PVDF membrane and P/E blended membrane with an EVOH/PVDF mass ratio of 1/9 at different temperatures of the coagulation bath. It is seen that the contact angle of the P/E blended

Table 1. Comparison of the water contact angles of the PVDF membrane and P/E blended membrane at different temperatures of the coagulation bath.

Temperature of the coagulation bath (°C)	0	20	40	60
P/E blended membrane (°)	80.3	60.4	56.4	71.6
PVDF membrane (°)	82.6	80.3	75.4	74.2

membrane was lower than that of the PVDF membrane at each tested temperature, demonstrating that the hydrophilicity was effectively improved by blending EVOH into the PVDF membrane. This is because there is a high density of (hydrophilic) hydroxyls in the EVOH chains,¹⁷ while PVDF is a highly hydrophobic polymer. The hydrophilic EVOH would have migrated spontaneously to the membrane surface during the phase inversion, thus improving the hydrophilicity of the membrane surface.

In addition, with an increase in the temperature of the coagulation bath, the contact angle of the P/E blended membrane initially decreased dramatically to a minimum and then increased, while the contact angle of the PVDF membrane decreased slightly. The different behaviors may be due to differences in the mechanism of the migration of EVOH to the membrane surface and the accumulation of

EVOH at the membrane surface at different bath temperatures. At 0 °C, the speed of phase separation of the P/E casting solution is lower, as is the rate of EVOH migrating to the membrane surface, thus resulting in a uniform distribution of EVOH in the cross section of the P/E blended membrane and little improvement in hydrophilicity. With an increase in the temperature of the coagulation bath, the migration of hydrophilic EVOH to the membrane surface accelerated during the membrane formation and the accumulated mass of EVOH on the membrane surface increased, thus reducing the membrane surface contact angle. However, when the temperature of the coagulation bath reaches 60 °C, there would be instantaneous demixing at the moment the PVDF/EVOH casting solution comes into contact with the coagulation bath, and the migration of hydrophilic EVOH to the membrane surface would be inhibited, thus increasing the contact angle of the blended membrane.

3.2.3. Effect of the temperature of the coagulation bath on the mechanical strength and permeation performance of blended membranes

The mechanical strength, pure-water flux and BSA rejection of the PVDF/EVOH (9/1 P/E mass ratio) blended membrane prepared at different temperatures of the coagulation bath are shown in Fig. 5.

It is seen that BSA rejection by the P/E blended membrane exceeded 90% and increased slightly with an increase in the temperature of the coagulation bath. When the temperature of the coagulation bath was 0 and 20 °C, the pure-water flux of the P/E blended membrane was 250 and 230 L/m²·h, respectively. However, the pure-water flux of the P/E blended membrane declined sharply when the temperature of the coagulation bath reached 40 °C, and it declined to a minimum (45 L/m²·h) when the temperature of the coagulation bath reached 60 °C. The changes in surface morphology and

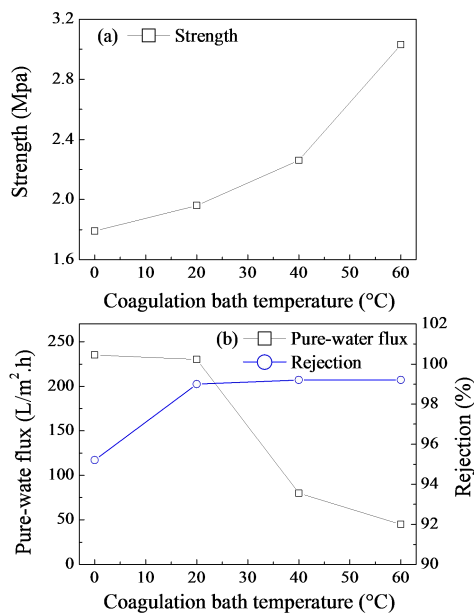


Figure 5. Mechanical strength (a), pure-water flux and BSA rejection (b) of blended membranes prepared at different temperatures of the coagulation bath.

contact angle as functions of temperature of the coagulation bath show that the pore size, pore density and hydrophilicity of the P/E blended membrane deteriorate at a coagulation bath temperature of 60 °C, resulting in a sharp decline in the pure-water flux with an increase in the temperature of the coagulation bath.

The mechanical strength of the P/E blended membrane increased with an increase in the temperature of the coagulation bath. This can be explained by the formation of a denser and less porous top layer at a higher bath temperature, as was well demonstrated by the surface morphology. Moreover, because the mechanical strength reflects compatibility between polymers to some degree, the excellent mechanical strength of the P/E blended membrane at higher coagulation bath temperatures demonstrated good compatibility between PVDF and EVOH at higher bath temperatures.

The above analysis reveals that the temperature of the coagulation bath should be fixed at 20 °C for optimum overall performance, including pore size, hydrophilicity, pure-water flux and BSA rejection.

3.3. Fouling test of the P/E blended membrane

Recently, many research groups have demonstrated that the measurement of adhesion forces of a membrane foulant by AFM in conjunction with a colloidal probe is a powerful method of assessing and unraveling membrane fouling behavior.^{30–32} To investigate the antifouling property of the P/E blended membrane, fouling experiments were conducted with PVDF membranes and P/E blended membranes, and the corresponding interaction forces between the membrane and foulant were investigated. All P/E blended membranes were prepared with a P/E mass ratio of 9/1 and in a coagulation bath at 20 °C.

3.3.1. Fouling experiments with PVDF and P/E blended membranes

Curves of the decline in normalized flux of PVDF and P/E blended membranes as a function of the filtration time for SA and HA solutions are depicted in Fig. 6. Note that the rate and

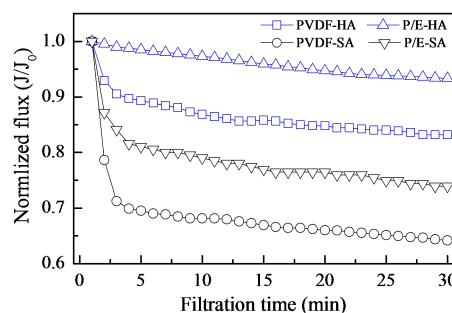


Figure 6. Relative flux of PVDF and P/E blended membranes as a function of filtration time for HA and SA solutions.

extent of the flux decline of PVDF membranes were higher than those of P/E blended membranes for both the SA solution and the HA solution. This suggests that the antifouling property of the PVDF membrane was effectively improved by blending EVOH into the membrane.

Furthermore, using either the PVDF membrane or P/E blended membrane, the flux decline rate of the SA-fouled membrane was much higher than that of the HA-fouled membrane. In particular, the relative flux (J/J_0) of the SA-fouled PVDF membrane decreased rapidly within the first 10 min of filtration and reached a minimum of 0.64. This decline was much greater in terms of the rate and extent of the relative flux decline than the declines for HA- and SA-fouled P/E blended membranes and HA-fouled PVDF membranes in the same filtration stage. This may be explained by the differences in the hydrogen-bonding interaction force between the membrane and the foulant. SA is rich in hydroxyl ions and is protonated at $\text{pH } 7.0 \pm 0.2$. It is easy to generate a hydrogen bond between the fluoride atoms (the most electronegative atoms) from the PVDF and the H atom from the hydroxyl group.³² This would accelerate the adsorption and accumulation of SA on the membrane surface or membrane pores and result in a sharp decline in flux.³³ The following studies were carried out to investigate the interaction forces between membrane and foulant and thus further confirm the above observation.

3.3.2. Characteristics of adhesion forces between membrane and foulant

In this study, hydroxyl and carboxyl colloidal probes were used as surrogates of SA and HA, which in conjunction with AFM were used to measure the interaction forces between the membrane (PVDF or P/E blended membrane) and colloidal probe; results are shown in Fig. 7. The negative values reflect the direction of the adhesive force. Consequently, in subsequent sections, the absolute value of the adhesive force is used.

The average adhesion forces of PVDF–carboxyl and P/E–carboxyl interactions were 4.73 and 3.31 $\text{mN}\cdot\text{m}^{-1}$, respectively, while the average adhesion forces of PVDF–

ARTICLE

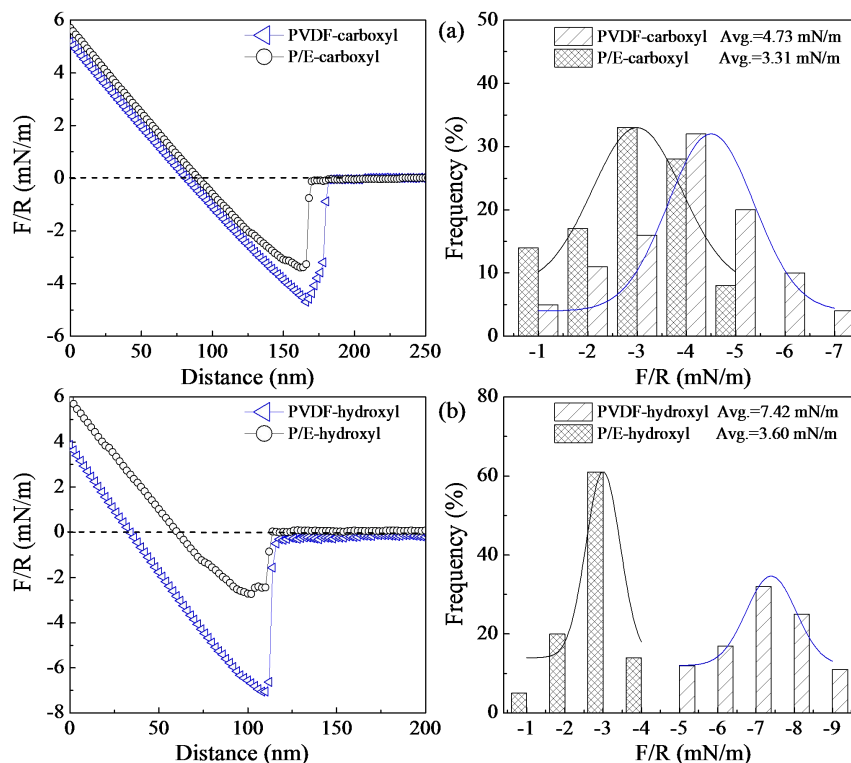


Figure 7. Representative normalized adhesion force versus distance of (a) the membrane-carboxyl interaction and (b) the membrane-hydroxyl interaction and the frequency distribution of corresponding forces.

hydroxyl and P/E-hydroxyl interactions were 7.42 and 3.6 $\text{mN}\cdot\text{m}^{-1}$, respectively. It is observed that the force of the PVDF-hydroxyl (or carboxyl) interaction was stronger than the force of the P/E-hydroxyl (or carboxyl) interaction. This may be because the PVDF membrane has a high density of fluoride atoms, which are the most electronegative atoms on the membrane surface and readily form a strong hydrogen bond with the hydrogen atoms from the hydroxyl or carboxyl group.²⁰ In contrast, the distribution density of fluoride atoms on the P/E blended membrane surface would be reduced by the aggregation of EVOH at the membrane surface, which would weaken the hydrogen bond interaction (mentioned above) between the membrane surface and the hydroxyl or carboxyl group.

In addition, for both the PVDF membrane and the P/E blended membrane, the membrane-carboxyl interaction force was weaker than the membrane-hydroxyl interaction force. This may be due to the fact that the pK_a values of hydroxyl and carboxyl groups correspond to $\text{pH} > 8$ and $\text{pH} = 3-6$, respectively.³⁴ The pK_a value is closely related to the bonding power of a hydrogen bond.³² In this study, fouling experiments and force measurements were performed with feed solutions of $\text{pH} 7.0 \pm 0.2$. Obviously, in this range, the carboxyl groups were almost completely deprotonated, while

hydroxyl groups were protonated. The protonated hydroxyl groups readily formed a strong hydrogen bond with the electronegative atoms from the membrane surface, which resulted in the membrane-hydroxyl adhesion force being stronger than the membrane-carboxyl interaction force.

The above phenomenon suggests that the antifouling ability of the P/E blended membrane is superior to that of the PVDF membrane. This is mainly because the interaction force between membrane and foulants was weakened by blending the EVOH into the PVDF membrane, which could mitigate the adsorption and accumulation of foulant in the surface and pores of the membrane. This is also the reason why the rate and extent of the flux decline of P/E blended membranes were lower than those of the PVDF membrane.

4. Conclusions

On the basis of complementing the respective chemical properties of PVDF and EVOH, PVDF/EVOH blended membranes were successfully synthesized by immersion precipitation, and the effects of the P/E mass ratio on the properties of the membranes were investigated. The hydrophilicity, pure-water flux and BSA rejection of blended membranes increased as the P/E mass ratio

changed from 20/0 to 9/1, which is mainly attributed to enhancement of the hydrophilic EVOH's migration to and accumulation at the membrane surface with an increase in EVOH content, leading to a denser and more hydrophilic EVOH top layer in the blended membranes. However, the BSA rejection and mechanical strength of the P/E blended membrane declined sharply when the P/E mass ratio reached 17/3 as the compatibility between PVDF and EVOH worsened. The optimum P/E mass ratio is 9/1 when taking the properties of membranes with different EVOH contents into account.

The temperature of the coagulation bath affected the surface morphology and properties of the blended membranes. With an increase in bath temperature, a denser and less porous top skin layer formed, which reduced the pure-water flux, membrane surface pore size and pore density, and increased the BSA rejection and mechanical strength. However, with an increase in bath temperature, the hydrophilicity of the P/E blended membrane initially decreased dramatically to a minimum and then increased. This is mainly explained by the difference in the speed of the EVOH migrating to the membrane surface and the accumulation mass of EVOH on the membrane surface. Following a comprehensive analysis of the properties of P/E blended membranes produced at different temperatures of the coagulation bath, an optimal bath temperature of 20 °C is proposed.

Comparing the P/E blended membrane prepared under the optimized condition (P/E mass ratio of 9/1 and coagulation bath temperature of 20 °C with a PVDF membrane, the pure-water flux increased from 160 to 230 L/m²·h, the BSA rejection increased from 94% to 99% and the surface contact angle decreased from 80.3° to 60.4°, while good mechanical strength was maintained. The overall performance of the P/E blended membrane was superior to that of the PVDF membrane.

During fouling experiments, the rate and extent of the flux decline of the P/E blended membrane were obviously less than those for the PVDF membrane. Moreover, further research on the interaction forces between the membrane (P/E blended membrane or PVDF membrane) and foulants confirmed that the antifouling ability of P/E blended membranes was superior to that of PVDF membranes. The membrane–foulant interaction forces were weakened by blending EVOH into the PVDF membrane, which could mitigate the adsorption and accumulation of foulant in the surface and pores of the membrane, resulting in a lower rate and extent of flux decline.

Acknowledgments

Financial support for this study was provided by the National Natural Science Foundation of China (Grant Nos 51178378 and 51278408), the Shanxi Province Science and Technology Innovation Projects (Grant Nos 2012KTCL03-06 and 2013KTCL03-16), the Foundation of the Shanxi Educational Committee (Grant No. 2013JK0884) and the Doctorate Foundation of Xi'an University of Architecture and Technology (Grant No. DB03154).

Corresponding Author

School of Environmental & Municipal Engineering, Xi'an University of Architecture and Technology, Yan Ta Road. No.13, Xi'an, China; *Lei Wang, Fax: +8602982202729; Tel: +8602982202729; E-mail: wanglei@xauat.edu.cn.

Notes

The authors declare no competing financial interest.

References

- 1 E. Filloux, J. Labanowski, J. Croue, *Bioresource Technology*, 2012, **118**, 460–468.
- 2 L. Farias, J. Howe, M. Thomson, *Water Research*, 2014, **58**, 102–110.
- 3 J. Tian, M. Ernst, F. Cui, M. Jekel, *Water research*, 2013, **47**, 1218–1228.
- 4 J. Tian, M. Ernst, F. Cui, M. Jekel, *Journal of Membrane Science*, 2013, **446**, 1–9.
- 5 Y. Zhang, J. Zhao, H. Chu, X. Zhou, Y. Wei, *Desalination*, 2014, **344**, 71–78.
- 6 N. Pezeshk, D. Rana, R. Narbaitz, T. Matsuura, *Journal of Membrane Science*, 2012, 389, 280–286.
- 7 Y. Wei, H. Chu, B. Dong, X. Li, S. Xia, Z. Qiang, *Desalination*, 2011, **272**, 90–97.
- 8 L. Shao, Z. Wang, Y. Zhang, Z. Jiang, Y. Liu., *Journal of Membrane Science*, 2014, **461**, 10–21.
- 9 C. Zhao, X. Xu, J. Chen, F. Yang, *Journal of Environmental Chemical Engineering*, 2013, **1**, 349–354.
- 10 E. Yuliwati, A. Ismail, *Desalination*, 2011, **273**, 226–234.
- 11 S. Liang, G. Qi, K. Xiao, J. Sun, E. Gianneli, X. Huang, M. Elimelech, *Journal of Membrane Science*, 2014, **463**, 94–101.
- 12 G. Kang, Y. Cao, *Journal of Membrane Science*, 2014, **463**, 145–165.
- 13 N. Ochoa, M. Masuelli, J. Marchese, *Journal of Membrane Science*, 2003, **226**, 203–211.
- 14 M. Masuelli, J. Marchese, N. Ochoa, *Journal of Membrane Science*, 2009, **326**, 688–693.
- 15 W. Lang, Z. Xu, H. Yang, W. Tong, *Journal of Membrane Science*, 2007, **288**, 123–131.
- 16 N. Riyasudheen, A. Sujith, *Desalination*, 2012, **294**, 17–24.
- 17 J. Lima, M. Felisberti, *Journal of Membrane Science*, 2009, **344**, 237–243.
- 18 J. Lima, M. Felisberti, *European Polymer Journal*, 2008, **44**, 1140–1148.
- 19 F. Liu, N. Hashim, Y. Liu, M. Abed, K. Li, *Journal of Membrane Science*, 2011, **375**, 1–27.
- 20 Israelachvili, J.N., 2011. *Intermolecular and Surface Forces*, third ed. Academic Press, London, p. 660.
- 21 L. Wang, R. Miao, X. Wang, Y. Lv, X. Meng, Y. Yang, D. Huang, L. Feng, Z. Liu, K. Ju, *Environment Science & Technology*, 2013, **47**, 3708–3714.
- 22 K. Katsoufidou, D. Sioutopoulos, S. Yiantsios, A. Karabelas, *Desalination*, 2010, **264**, 220–227.

- 23 E. Celik, H. Park., H. Choi, H. Choi, *Water Research*, 2011, **45**, 274–282.
- 24 G. Arthanareeswaran, P. Thanikaivelan, *Separation and Purification Technology*, 2010, **74**, 230–235.
- 25 C. Xu, W. Huang, X. Lu, D. Yan, S. Chen, H. Huang, *Radiation Physics and Chemistry*, 2012, **81**, 1763–1769.
- 26 J. Yu, L. Zhu, B. Zhu, Y. Xu, *Journal of Membrane Science*, 2011, **366**, 176–183.
- 27 A. Conesa, T. Gum, C. Palet, *Journal of Membrane Science*, 2007, **287**, 29–40.
- 28 S. Singh, K. Khulbe, T. Matsuura, P. Ramamurthy, *Journal of Membrane Science*, 1998, **142**, 111–127.
- 29 Y. Guo, X. Feng, L. Chen, Y. Zhao, J. Bai, *Journal of Applied Polymer Science*, 2010, **116**, 1005–1009.
- 30 Q. Li, M. Elimelech, *Environment Science & Technology*, 2004, **38**, 4683–4693.
- 31 C. Tang, Y. Kwon, J. Leckie, *Journal of Membrane Science*, 2009, **326**, 526–532.
- 32 H. Yamamura, K. Kimura, T. Okajima, H. Tokumoto, Y. Watanabe, *Environment Science & Technology*, 2008, **42**, 5310–5315.
- 33 R. Miao, L. Wang, Y. Lv, X. Wang, L. Feng, Z. Liu, D. Huang, Y. Yang, *Water Research*, 2014, **55**, 313–322.
- 34 S. Lee, M. Elimelech, *Environment Science & Technology*, 2006, **40**, 980–987.